Input Current Characteristics of a Three-Phase Diode Rectifier with Capacitive Filter Under Line Voltage Unbalance Condition

Seung-Gi Jeong, Dong-Ki Lee
Dept of Electrical Engineering, Kwangwoon University, Seoul, Korea
sgjeong@daisy.kwangwoon.ac.kr

Ki-Won Park
POSCON, Seoul, Korea
kwpark@poscon.co.kr

Abstract

The three-phase diode rectifier with a capacitive filter is highly sensitive to line voltage unbalance, and may cause significantly unbalanced line currents even under slightly unbalanced voltage condition. This paper presents an analysis of this 'unbalance amplification' effect for an ideal rectifier circuit without ac- and dc-side inductors. The voltage unbalance is modeled by introducing a deviation voltage superimposed on balanced three-phase line voltages. With proper approximations, closed-form expressions for symmetrical components of the line current and current unbalance factor are derived in terms of the voltage unbalance factor, filter reactance, and load current. The validity of analytical predictions is confirmed by simulation.

Keywords: uncontrolled rectifier, diode rectifier, voltage unbalance, current unbalance, power quality

I. INTRODUCTION

As vast majority of modern power converters are supplied from ac lines via uncontrolled diode rectifiers, the input line current characteristics of diode rectifiers have significant impacts on power quality. Unfortunately, the diode rectifiers are not friendly to supply lines due to their highly nonlinear nature. Most diode rectifiers are accompanied by large smoothing dc capacitors that shorten the conduction period of rectifying devices, resulting in pulse-shaped line current rich in harmonics.

In three-phase rectifiers, not only the harmonics but also the unbalance of input current is one of primary concerns in field applications. As the smoothing capacitor keeps dc voltage very close to the peak of line-to-line voltage, the current flows over brief periods to charge the capacitor in the vicinity of line voltage peaks. Therefore, a slight variation of the voltage peak in some phase(s), or a small voltage unbalance may cause a significant variation in line current waveforms, that is, highly unbalanced line currents. Similar 'unbalance amplification' is observed in induction motor drives where negative-sequence impedance is much smaller than positive-sequence impedance, yielding the current several times more unbalanced than the line voltage. Diode rectifiers, however, are far more sensitive to the voltage unbalance due to their nonlinear behavior under unbalanced voltage supply. As a result, it is not uncommon to encounter rectifier currents significantly unbalanced even when the supply voltage unbalance is well below a usually acceptable level.

Unbalanced rectifier currents cause detrimental effects including: Uneven current distribution over the legs of the rectifier bridge that increases the conduction loss and may cause failure of rectifying devices; Increased RMS ripple current in the smoothing capacitor; Increased total RMS line current and harmonics, in particular, non-characteristic triplen harmonics that do not appear under balanced condition [1-3].

As most industrial and commercial power lines are more or less unbalanced, care should be taken in designing and installing diode rectifiers to keep the current unbalance within an acceptable level, and to avoid the above undesirable effects. Although the effects have been well recognized in field applications [1, 4-6], only a few works have been devoted to the theoretical investigation of the input current characteristics of a diode rectifier under unbalanced voltage condition. Some analytical approaches can be found in [2], [3], and [7], but they assume continuous dc current to examine third harmonic characteristics, which seems not to be valid in frequently encountered discontinuous current operation.

This paper is intended to establish a basic relationship between the voltage unbalance and the current unbalance of a three-phase diode rectifier. To attain a better physical understanding, an analytical approach is made. The effects of ac- and dc-side inductors are neglected, to ease the analysis and to give a worst-case figure of current unbalance.

II. REPRESENTATION OF VOLTAGE UNBALANCE

The most popular way of representing the voltage unbalance is the maximum percent deviation of line voltages from their average value. Although this definition is simple and useful in field applications, it is not suitable for analytical purpose nor adequate to properly represent various unbalance conditions. Therefore, in the following analysis, the voltage unbalance factor defined with symmetrical components is used, which is expressed in a complex form

$$\mathbf{u} = ue^{j\theta} = \frac{\mathbf{V}_n}{\mathbf{V}_p} \tag{1}$$

where

$$\begin{bmatrix}\mathbf{V}_p\\ \mathbf{V}_n\\ \mathbf{V}_z\end{bmatrix} = \frac{1}{3}\begin{bmatrix}1 & \mathbf{a} & \mathbf{a}^2\\ 1 & \mathbf{a}^2 & \mathbf{a}\\ 1 & 1 & 1\end{bmatrix}\begin{bmatrix}\mathbf{V}_{ab}\\ \mathbf{V}_{bc}\\ \mathbf{V}_{ca}\end{bmatrix} \qquad (\mathbf{a} = e^{j\frac{2\pi}{3}}). \tag{2}$$

It should be noted that (2) is defined with line-to-line voltages instead of phase voltages, considering that the rectifier behavior is more effectively described with line-to-line voltages. As a natural consequence, the zero-sequence component, $\mathbf{V}_z$, is trivially zero.

In order to evaluate current unbalance, the line voltages should be determined first for given voltage unbalance condition. This requires an inverse relationship of (1) and (2). The relationship can be derived by introducing the voltage deviation ΔV superimposed on a balanced set of line voltages, that is,

$$\begin{aligned}\mathbf{V}_{ab} &= V\\ \mathbf{V}_{bc} &= \mathbf{a}^2 V + \Delta\mathbf{V}.\\ \mathbf{V}_{ca} &= \mathbf{a}V - \Delta\mathbf{V}\end{aligned} \tag{3}$$

In the above expressions, $\mathbf{V}_{ab}$ is taken as a reference phasor fixed on the real axis, and its magnitude, V, is the nominal rms line-to-line voltage. Substituting (3) into (2) results in the positive- and negative-sequence voltage as

$$\mathbf{V}_p = V + j\frac{1}{\sqrt{3}}\Delta\mathbf{V} \tag{4}$$

$$\mathbf{V}_n = -j\frac{1}{\sqrt{3}}\Delta\mathbf{V}. \tag{5}$$

Substituting (4) and (5) into (1) yields the deviation voltage expressed in terms of the voltage unbalance factor as

$$\Delta\mathbf{V} = j\sqrt{3}\frac{\mathbf{u}}{1+\mathbf{u}}V. \tag{6}$$

With the above equation, the line voltages in (3) can be determined for given unbalance factor, while associated symmetrical components are given by

$$\mathbf{V}_p = \frac{1}{1+\mathbf{u}}V \tag{7}$$

$$\mathbf{V}_n = \frac{\mathbf{u}}{1+\mathbf{u}}V \tag{8}$$

The above relationships show that not only the magnitude but also the argument of the voltage unbalance factor needs to be specified to determine the line voltages. When only the magnitude of the voltage unbalance is given, the symmetrical components and the line voltages can be obtained as follows.

Writing down the negative-sequence voltage explicitly,

$$\mathbf{V}_n = V_x + jV_y \tag{9}$$

and accordingly, from (4) and (5),

$$\mathbf{V}_p = V - \mathbf{V}_n = V - V_x - jV_y \tag{10}$$

gives the voltage unbalance ratio

$$u = \frac{V_n}{V_p} = \frac{\sqrt{V_x^2 + V_y^2}}{\sqrt{(V - V_x)^2 + V_y^2}}. \tag{11}$$

It can be shown that (11) reduces to

$$\left(V_x + \frac{u^2}{1-u^2}V\right)^2 + V_y^2 = \left(\frac{u}{1-u^2}V\right)^2 \tag{12}$$

which shows that, for given unbalance factor, the phasor of the negative-sequence component lies on a circle. As the deviation voltage is proportional to the negative-sequence voltage, the phasors of the unbalanced line voltages also draw circles as illustrated in Fig. 1.

The phasor loci in Fig. 1 are drawn for 20% voltage unbalance factor. In normal operating conditions, however, the voltage unbalance is usually restricted to be less than 2-3%. Under these circumstances, (6)-(8) reduces to

$$\Delta\mathbf{V} \approx j\sqrt{3}\mathbf{u}V \tag{13}$$

$$\mathbf{V}_p \approx V \tag{14}$$

$$\mathbf{V}_n \approx \mathbf{u}V. \tag{15}$$

Eq. (15) indicates that the phasor locus of the negative-sequence voltage is centered very closely to the origin and has the radius proportional to the voltage unbalance factor. Accordingly, the loci of line voltages are approximately centered at their balanced phasor locations for a few per cent voltage unbalance factor.

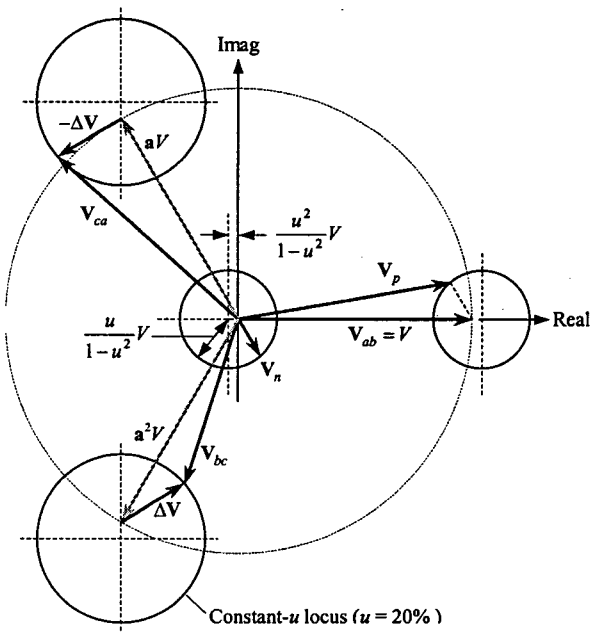

Fig. 1 Phasor loci of symmetrical components and line voltages for given voltage unbalance factor

III. OPERATING MODES OF RECTIFIER UNDER UNBALANCED VOLTAGE CONDITION

Fig. 2 shows a three-phase diode rectifier circuit with a capacitor filter. For simplicity, the load is supposed to be a constant current sink of I_L, and the effects of line side inductance are not considered ($L = 0$). Fig. 3 shows the voltage and current waveforms of the rectifier circuit under balanced condition. In the rectifier output, six line voltages appear sequentially as indicated in the figure. In the vicinity of peak of each line voltages, a brief charging period appears and is followed by a discharging period that approaches to 60 degrees as the capacitor becomes large and/or the load current decreases. The voltage droop during the discharging period is approximately given by

$$V_r \approx \frac{\pi}{3}\frac{I_L}{\omega C} = \frac{\pi}{3}X_C I_L \tag{16}$$

where X_C is the reactance of the filter capacitor at line frequency. When balanced, V_r represents the peak-to-peak ripple of the rectifier output, to give the ripple factor defined as

$$\rho = \frac{V_r}{\sqrt{2}V} \tag{17}$$

which is referred to the 'voltage droop ratio' in the following. The voltage droop ratio represents combinational effects of the load current and filter capacitance in describing the behavior of the rectifier under unbalanced voltage condition.

When unbalanced, the peaks of the line voltages are not uniform, but fluctuate periodically over a cycle. Fig. 4 shows the deviated six line voltages where $\mathbf{V}_{ac}$ and $\mathbf{V}_{bc}$ are deviated by $\Delta\mathbf{V}$ while $\mathbf{V}_{ca}$ and $\mathbf{V}_{cb}$ deviated by $-\Delta\mathbf{V}$. In time axis, the variation of the peak voltages over a half cycle appears as shown in Fig. 5. It is clear from Fig. 4 that the same variation repeats every half cycle.

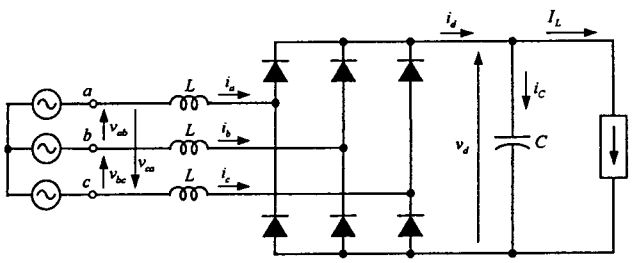

Fig. 2 Three-phase diode rectifier

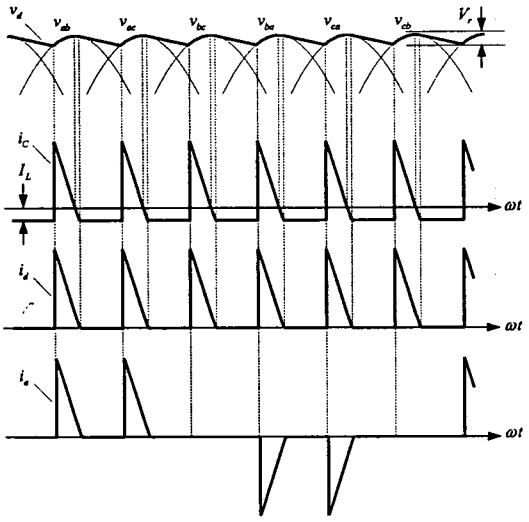

Fig. 3 Rectifier waveforms of balanced operation

Fig. 5 assumes a small voltage unbalance factor so that the center of a circle coincides the peak of the reference balanced voltage. The radius of the circles in Fig. 5 is given by

$$\Delta\hat{V} = \sqrt{6}uV . \tag{18}$$

Therefore, the unbalanced peak voltages varies in the range of $\sqrt{2}V \pm \Delta\hat{V}$ according to the phase angle of the deviation voltage, ϕ. The position of the peak voltages in time axis also varies, however, the effect of the phase shift is neglected to avoid complication.

Under the assumption of small charging period, the variation of the output voltage of the rectifier over a cycle can be represented as a pulse train shown in Fig. 6. In view of Fig. 5, the peak line voltages are given by

$$\sqrt{2}V_{ab} = \sqrt{2}V \tag{19}$$

$$\sqrt{2}V_{bc} = \sqrt{2}V + \Delta\hat{V}\cos(\phi+\gamma) \tag{20}$$

$$\sqrt{2}V_{ca} = \sqrt{2}V - \Delta\hat{V}\cos(\phi-\gamma) \tag{21}$$

where $\gamma = 2\pi/3$.

As shown in Fig. 6, there are three distinct modes of operation. In Fig. 6(a), all six peak voltages appear in the rectifier output, causing six charging period over a cycle, which is referred to 6-pulse mode of operation. In Fig. 6(b), two peak voltages are submerged below the rectifier output voltage resulting in a 4-pulse mode of operation. If one of the three line voltages is significantly larger than the others, then only two charging period appears as in Fig. 8(c), resulting in the 2-pulse mode of operation.

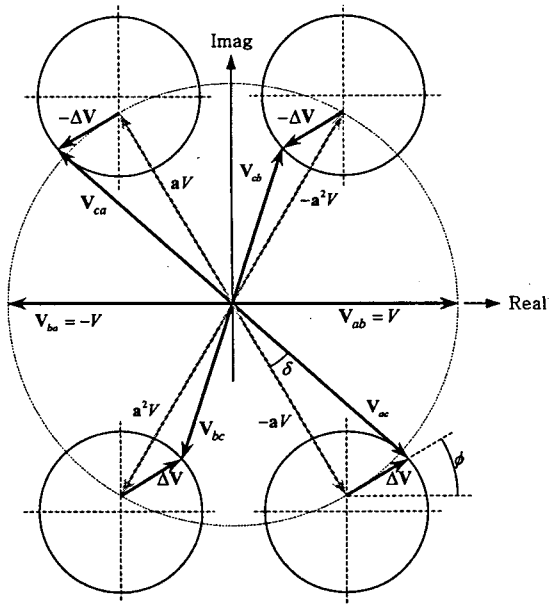

Fig. 4 Unbalanced line voltage phasors that appear at the rectifier output

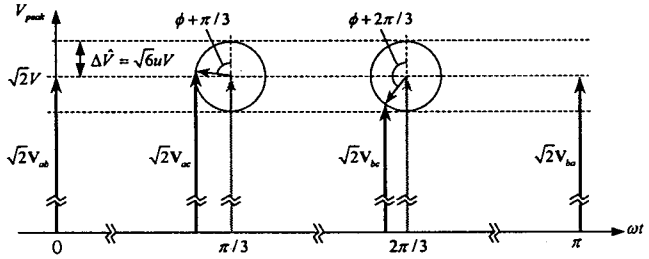

Fig. 5 Variation of line-to-line peak voltages in time axis

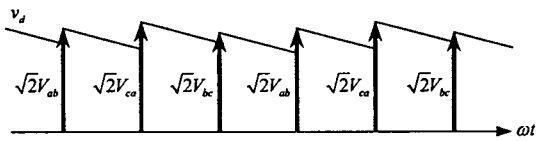

(a) 6-pulse mode

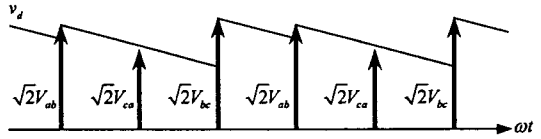

(b) 4-pulse mode

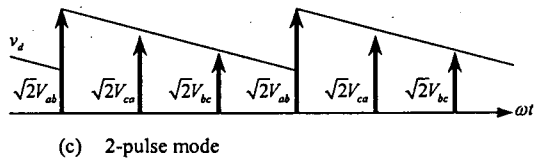

(c) 2-pulse mode

Fig. 6 Operation modes under unbalanced condition

The 4-pulse mode is further divided into three different operating modes according to which line voltages appear in the rectifier output. For instance, Fig. 6(b) shows the case of $\mathbf{V}_{ab}$ and $\mathbf{V}_{bc}$ active in the rectifier output, which is referred to the *ab-bc* mode in the following. The *bc-ca* mode and the *ca-ab* mode are defined in a similar manner. The 2-pulse mode is also divided into three modes: *ab, bc,* and *ca* mode

where only V_{ab}, V_{bc}, and V_{ca} appears in the output, respectively. Therefore, there are seven different modes of operation in total.

Which mode the rectifier operates in depends on the degree of voltage unbalance, phase angle of the deviation voltage, and the voltage droop during the discharging period (V_r). For example, by examining Fig. 6(b), the condition for *ab-bc* mode of operation is given by

$$\sqrt{2}V_{ab} - V_r > \sqrt{2}V_{ca} \tag{22}$$

$$\sqrt{2}V_{ab} - 2V_r < \sqrt{2}V_{bc} \tag{23}$$

$$\sqrt{2}V_{bc} - V_r < \sqrt{2}V_{ab} \tag{24}$$

If (23) does not hold, then V_{bc} will be submerged, giving the condition for the *ab* mode of operation as

$$\sqrt{2}V_{ab} - V_r > \sqrt{2}V_{ca} \tag{25}$$

$$\sqrt{2}V_{ab} - 2V_r > \sqrt{2}V_{bc} \tag{26}$$

The conditions for all seven modes can be established in a similar way. With (16), (17) and (19)-(21), it can be shown that the conditions reduce to the following relationships between the voltage droop ratio, voltage unbalance factor, and the phase angle of the deviation voltage:

ab-bc-ca mode (6-pulse)

$$\rho > u_0 \text{ and } \rho > u_1 \text{ and } \rho > u_2 \tag{27}$$

ab-bc mode

$$\rho < u_1 \text{ and } \rho > -u_2/2 \text{ and } \rho > u_2 \tag{28}$$

bc-ca mode

$$\rho < u_2 \text{ and } \rho > -u_0/2 \text{ and } \rho > u_0 \tag{29}$$

ca-ab mode

$$\rho < u_0 \text{ and } \rho > -u_1/2 \text{ and } \rho > u_1 \tag{30}$$

ab mode

$$\rho < u_1 \text{ and } \rho < -u_2/2 \tag{31}$$

bc mode

$$\rho < u_2 \text{ and } \rho < -u_0/2 \tag{32}$$

ca mode

$$\rho < u_0 \text{ and } \rho < -u_1/2 \tag{33}$$

where

$$u_0 = \sqrt{3}u\cos\phi \tag{34}$$

$$u_1 = \sqrt{3}u\cos(\phi - \gamma) \tag{35}$$

$$u_2 = \sqrt{3}u\cos(\phi + \gamma) \tag{36}$$

Fig. 7 shows the operation modes in the plane of complex voltage unbalance factor. Six solid lines divide the whole area into seven regions each corresponds to one of the operation modes described above. The triangle at the center represents the 6-pulse region given by (27). The circle inscribing the triangle corresponds to $u = \rho/\sqrt{3}$, or $|\Delta V| = \rho V$. If the voltage unbalance factor is less than this value, the rectifier operates in 6-pulse mode regardless of the phase of the deviation voltage. And above this value, the rectifier operates in 6-pulse or 4-pulse mode, depending on the phase of the deviation voltage. This holds until the voltage unbalance factor reaches $u = 2\rho/\sqrt{3}$ which is indicated by the circle circumscribing the triangle. Further increase of voltage unbalance will make the rectifier to operate in 2-pulse or 4-pulse mode. The larger the voltage unbalance factor is, the narrower the region of phase angle of deviation voltage for 4-pulse mode of operation. But at the phase angles of 30°, 150° and -90° the 2-pulse mode never occurs. And at the phase angles of 60°, 180° and -60° the 4-pulse mode never occurs.

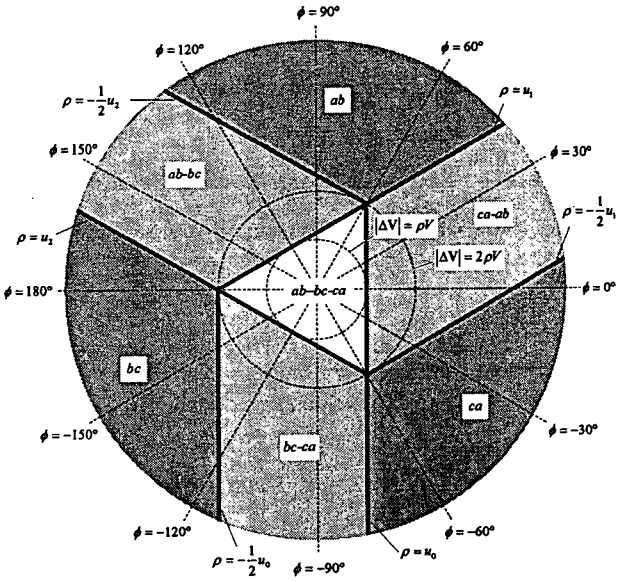

Fig. 7 Operation modes in the complex unbalance factor plane

IV. LINE CURRENT UNBALANCE IN 6-PULSE MODE

The waveform of i_d in Fig. 3 is composed of charging current pulses. Assuming short charging periods, the current-time area of a current pulse is approximately given by

$$A \approx \omega C \Delta V_d = \frac{\Delta V_d}{X_C} \tag{37}$$

where ΔV_d is the increment of the output voltage due to the charging current pulse.

To simplify the analysis, in the following, the current pulses are approximated to square pulses that have the same area with that of the actual current pulses. With this approximation, the dc and line side current waveforms in 6-pulse mode can be represented as shown in Fig. 8.

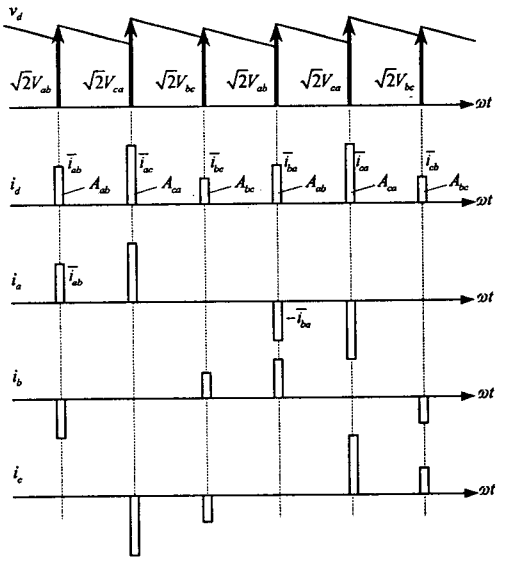

Fig. 8 Approximated line currents for six-pulse mode of operation

The subscripts of current pulses in the figure indicate associated active line voltages that appear at the output. Due to half-cycle symmetry, the current pulses $\bar{i}_{ab}$ and $\bar{i}_{ba}$ are of the same area, A_{ab}, and so on. Combining (37) and (19)-(21) gives the area of the current pulses as follows:

$$A_{ab} = \frac{1}{X_C}[V_r - \Delta\hat{V}\cos(\phi+\gamma)] \tag{38}$$

$$A_{bc} = \frac{1}{X_C}[V_r - \Delta\hat{V}\cos\phi] \tag{39}$$

$$A_{ca} = \frac{1}{X_C}[V_r - \Delta\hat{V}\cos(\phi-\gamma)] \tag{40}$$

The current pulses in i_d are distributed over three-phase line current, and each phase of the line currents appears to be a combination of two of three current pulse pairs, $\bar{i}_{ab} - (-\bar{i}_{ba})$, $\bar{i}_{bc} - (-\bar{i}_{cb})$, and $\bar{i}_{ca} - (-\bar{i}_{ca})$. A current pulse pair has the Fourier coefficient

$$a_n = \frac{4}{\pi}\frac{h}{n}\sin\frac{n\theta}{2} \tag{41}$$

where h and θ represent the magnitude and width of the current pulse, respectively. If $n\theta$ in (41) is sufficiently small, the Fourier coefficient is approximated to

$$a_n \approx \frac{2}{\pi}h\theta = \frac{2}{\pi}A \tag{42}$$

which is valid for low order harmonics, namely, the fundamental and third harmonic component.

Therefore, from (38)-(40), the fundamental component of the current pulse pairs are given by

$$I_{ab1} = \frac{\sqrt{2}}{\pi}A_{ab} = \frac{\sqrt{2}}{\pi}\frac{1}{X_C}[V_r - \Delta\hat{V}\cos(\phi+\gamma)] \tag{43}$$

$$I_{bc1} = \frac{\sqrt{2}}{\pi}A_{bc} = \frac{\sqrt{2}}{\pi}\frac{1}{X_C}[V_r - \Delta\hat{V}\cos\phi] \tag{44}$$

$$I_{ca1} = \frac{\sqrt{2}}{\pi}A_{ca} = \frac{\sqrt{2}}{\pi}\frac{1}{X_C}[V_r - \Delta\hat{V}\cos(\phi-\gamma)] \tag{45}$$

As the fundamental component due to $\bar{i}_{ab} - (-\bar{i}_{ba})$ pair is in-phase with the reference phasor $\mathbf{V}_{ab}$, the phasors of three-phase line currents are given by

$$\mathbf{I}_{a1} = I_{ab1} - \mathbf{a}I_{ca1} \tag{46}$$

$$\mathbf{I}_{b1} = \mathbf{a}^2 I_{bc1} - I_{ab1} \tag{47}$$

$$\mathbf{I}_{c1} = \mathbf{a}I_{ca1} - \mathbf{a}^2 I_{bc1} \tag{48}$$

which yield the symmetrical components

$$\mathbf{I}_{p1} = \frac{1}{3}(1-\mathbf{a})(I_{ab1} + I_{bc1} + I_{ca1}) \tag{49}$$

$$\mathbf{I}_{n1} = \frac{1}{3}(1-\mathbf{a}^2)(I_{ab1} + \mathbf{a}I_{bc1} + \mathbf{a}^2 I_{ca1}). \tag{50}$$

and the unbalance factor of fundamental current

$$\mu = \frac{\mathbf{I}_{n1}}{\mathbf{I}_{p1}} = \frac{\left|I_{ab1} + \mathbf{a}I_{bc1} + \mathbf{a}^2 I_{ca1}\right|}{I_{ab1} + I_{bc1} + I_{ca1}}. \tag{51}$$

By substituting (43)-(45) into (49)-(51), the symmetrical components and current unbalance factor are represented in terms of the line voltage deviation or the voltage unbalance factor. The positive-sequence current reduces to

$$\mathbf{I}_{p1} = (1-\mathbf{a})\frac{\sqrt{2}}{\pi}\frac{V_r}{X_C} \tag{52}$$

or, with (16),

$$\mathbf{I}_{p1} = (1-\mathbf{a})\frac{\sqrt{2}}{3}I_L = \sqrt{\frac{2}{3}}I_L e^{-j\pi/6}. \tag{53}$$

The negative-sequence current is

$$\mathbf{I}_{n1} = \frac{\sqrt{3}}{\sqrt{2}\pi}\frac{\Delta\hat{V}}{X_C}e^{j(\phi-\pi/6)} \tag{54}$$

or with (18),

$$\mathbf{I}_{n1} = \frac{3}{\pi}\frac{V}{X_C}ue^{j(\phi-\pi/6)} \tag{55}$$

Above expressions clearly show the effects of three parameters – the voltage unbalance factor (or the deviation voltage), the load current, and the reactance of the capacitor filter. The load current is reflected to only the positive-sequence current while the voltage unbalance factor has an effect on the negative-sequence current only.

The negative-sequence current is proportional to the voltage unbalance factor and inversely proportional to the filter reactance. With (15), the magnitude of negative-sequence current is related to the negative-sequence voltage as

$$I_{n1} = \frac{V_n}{(\pi/3)X_C} \tag{56}$$

which clearly shows that the negative-sequence impedance of the rectifier is solely determined by the capacitive filter reactance.

The expression of the current unbalance factor is, from (52) and (54), given by

$$\mu = \sqrt{\frac{3}{2}}\frac{V}{V_r}u \tag{57}$$

With the voltage droop ratio, defined in (17), above equation can be written down as

$$\frac{\mu}{u} = \frac{\sqrt{3}}{2}\frac{1}{\rho} \tag{58}$$

The voltage droop ratio, ρ, corresponds to the output voltage ripple factor in balanced case. As the ripple factor is usually limited to a few percent, the above equation indicates that the current unbalance is as large as several tens times the voltage unbalance, showing unbalance amplification effect, unless proper line side inductance is provided.

V. LINE CURRENT UNBALANCE IN 4- AND 2-PULSE MODE

Fig. 9 shows a 4-pulse mode of operation. Shown is the *ab-bc* mode where the current waveforms of phase *a* and phase *c* is similar to that of single-phase rectifier while only phase *b* carries four pulses per cycle. In this case, the pulse areas are given by

$$A_{ab} = \frac{1}{X_C}[V_r - \Delta\hat{V}\cos(\phi+\gamma)] \tag{59}$$

$$A_{bc} = \frac{1}{X_C}[2V_r + \Delta\hat{V}\cos(\phi+\gamma)] \tag{60}$$

which gives the magnitude of fundamental component of current pulse pairs:

$$I_{ab1} = \frac{\sqrt{2}}{\pi}A_{ab} = \frac{\sqrt{2}}{\pi}\frac{1}{X_C}[V_r - \Delta\hat{V}\cos(\phi+\gamma)] \tag{61}$$

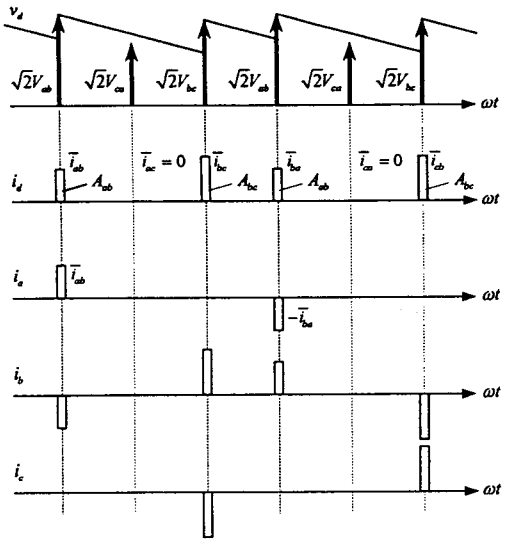

Fig. 9 Line currents in 4-pulse mode

$$I_{bc1} = \frac{\sqrt{2}}{\pi} A_{bc} = \frac{\sqrt{2}}{\pi} \frac{1}{X_C} [2V_r + \Delta\hat{V} \cos(\phi + \gamma)] \tag{62}$$

Comparing Fig. 9 with Fig. 8 shows that line current phasors and their symmetrical components in *ab-bc* mode can be obtained by simply removing I_{ca1} terms from 6-pulse case. Therefore,

$$\mathbf{I}_{p1} = \frac{1}{3}(1 - \mathbf{a})(I_{ab1} + I_{bc1}) \tag{63}$$

$$\mathbf{I}_{n1} = \frac{1}{3}(1 - \mathbf{a}^2)(I_{ab1} + \mathbf{a} I_{bc1}) \tag{64}$$

Similar procedure applies for *bc-ca* and *ca-ab* mode and it can be shown that the positive-sequence current is given by

$$\mathbf{I}_{p1} = (1 - \mathbf{a}) \frac{\sqrt{2}}{\pi} \frac{V_r}{X_C} = \frac{\sqrt{2}}{3} I_L e^{-j\pi/6} \tag{65}$$

which invariably holds for all 4-pulse modes.

The negative-sequence current, on the other hand, depends not only the magnitude but also the phase of the deviation voltage:

ab-bc mode ($\pi/3 \le \phi \le \pi$)

$$\mathbf{I}_{n1} = \frac{\sqrt{2}}{\pi} \frac{1}{X_C} \mathbf{a} [V_r - \mathbf{a}^2 \Delta\hat{V} \cos(\phi + \gamma)] \tag{66}$$

bc-ca mode ($-\pi/3 \le \phi \le \pi/3$)

$$\mathbf{I}_{n1} = \frac{\sqrt{2}}{\pi} \frac{1}{X_C} [V_r - \mathbf{a}^2 \Delta\hat{V} \cos(\phi + \gamma)] \tag{67}$$

ca-ab mode ($-\pi \le \phi \le -\pi/3$)

$$\mathbf{I}_{n1} = \frac{\sqrt{2}}{\pi} \frac{1}{X_C} \mathbf{a}^2 [V_r - \mathbf{a}^2 \Delta\hat{V} \cos(\phi + \gamma)] \tag{68}$$

From the above expressions, the current unbalance factor is given by

$$\mu = \sqrt{c^2 \left(\frac{u}{\rho}\right)^2 + \frac{1}{\sqrt{3}} c \frac{u}{\rho} + \frac{1}{3}} \tag{69}$$

where

$$c = \begin{cases} \cos(\phi + \gamma) & \pi/3 \le \phi \le \pi \\ \cos(\phi - \gamma) & -\pi/3 \le \phi \le \pi/3 \\ \cos\phi & -\pi \le \phi \le -\pi/3 \end{cases}$$

The 2-pulse mode of operation is illustrated in Fig. 10. The figure assumes the *ab*-mode wherein V_{ab} is the largest among the line voltages. Phase *c* does not conduct and the rectifier operates like a single-phase rectifier fed by V_{ab}.

The area of the current pulse is

$$A_{ab} = \frac{3V_r}{X_C} \tag{70}$$

to give the magnitude of the fundamental current as

$$I_{ab1} = \frac{\sqrt{2}}{\pi} A_{ab} = \frac{\sqrt{2}}{\pi} \frac{3V_r}{X_C} \tag{71}$$

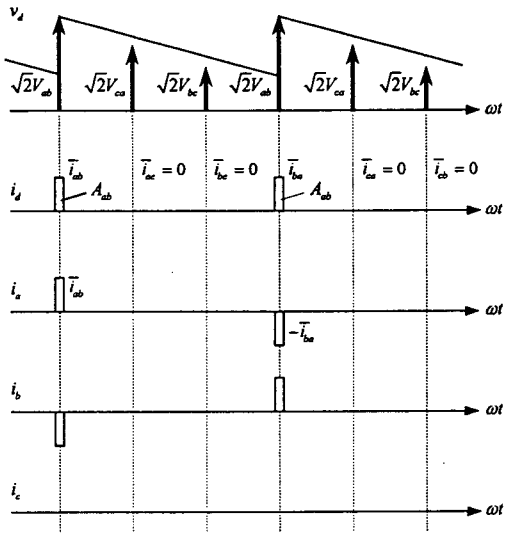

Fig. 10 Line currents in 2-pulse mode

Comparing Fig. 10 with Fig. 8 shows that line current phasors and their symmetrical components in *ab* mode can be obtained by removing I_{bc1} and I_{ca1} terms from 6-pulse case. Therefore,

$$\mathbf{I}_{p1} = \frac{1}{3}(1 - \mathbf{a}) I_{ab1} \tag{72}$$

$$\mathbf{I}_{n1} = \frac{1}{3}(1 - \mathbf{a}^2) I_{ab1} \tag{73}$$

The positive-sequence current in (72) reduces to the same expression as in 6- and 4-pulse mode, which holds for *bc* and *ca* mode as well. The magnitude of the negative-sequence current is the same with that of the positive-sequence current, independent of the voltage unbalance. For completeness, the negative-sequence current in all three 2-pulse modes is given below.

ab mode ($\pi/6 \le \phi \le 5\pi/6$)

$$\mathbf{I}_{n1} = \sqrt{2/3} I_L e^{j\pi/6} \tag{74}$$

bc mode ($\pi/6 \le \phi \le 9\pi/6$)

$$\mathbf{I}_{n1} = \sqrt{2/3} I_L \mathbf{a} e^{j\pi/6} \tag{75}$$

ca mode ($9\pi/6 \le \phi \le 13\pi/6$)

$$\mathbf{I}_{n1} = \sqrt{2/3} I_L \mathbf{a}^2 e^{j\pi/6} \tag{76}$$

And it is apparent that the current unbalance factor is

$$\mu = 1 \tag{77}$$

VI. CHARACTERISTICS OF UNBALANCED LINE CURRENT

With the expressions of symmetrical components given above, the phasor loci for various voltage unbalance factor are depicted in Fig. 11. The positive-sequence current is fixed in the complex plane as long as the dc load current is kept constant. As the negative-sequence current never exceeds the positive sequence current in magnitude, its phasor locus is constrained within the circle drawn with dashed lines. The negative-sequence current is further constrained within the triangle that inscribes the circle. Three corners of the triangle represent the phasor locations in 2-pulse mode given by (74)-(76), and the sides of the triangle represent the phasor locus in 4-pulse mode given by (66)-(68). The inside region of the triangle represents 6-pulse mode.

In 6-pulse mode operation, the negative-sequence current leads the positive-sequence current by the phase angle of the deviation voltage, drawing a circle for given voltage unbalance factor. For a voltage unbalance factor less than $\rho/\sqrt{3}$, the circle is well within the triangle and the rectifier operates in 6-pulse mode all over the phase angle. When $u = \rho/\sqrt{3}$, the locus inscribes the triangle and its radius is one-half the magnitude of the positive-sequence current, resulting in 50% current unbalance factor. For $\rho/\sqrt{3} < u < 2\rho/\sqrt{3}$, the negative-sequence phasor lies on a side of the triangle in 4-pulse mode or on a circle in 6-pulse mode, depending on its phase angle. For $u > 2\rho/\sqrt{3}$, the 6-pulse mode no more appears. The phasor is fixed at one of three corners of the triangle in 2-pulse mode and moves along the sides of the triangle in 4-pulse mode.

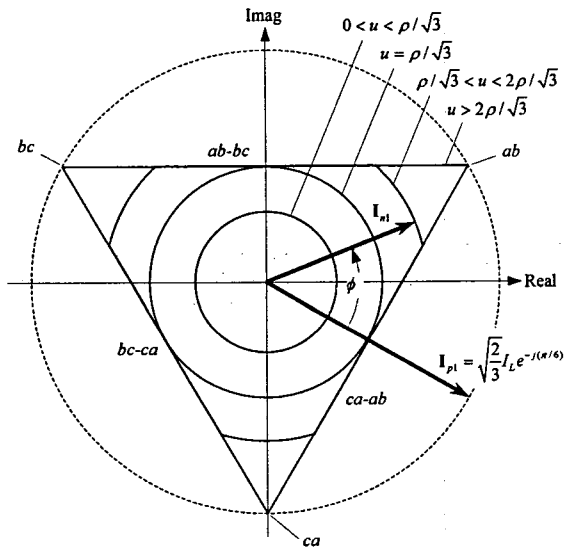

Fig. 11 Phasor of the positive-sequence current and phasor loci of the negative-sequence current

The variation of the current unbalance factor versus the voltage unbalance factor is plotted in Fig. 12, for the phase angle from 0° to 120°. The figure shows that, as the voltage unbalance factor increases, the current unbalance factor linearly increases from 0 to 50% and then varies in a rather complicated manner until it reaches to 100%. An exception is the case of $\phi = 30°$ where the current unbalance factor remains at 58%($1/\sqrt{3}$). This is because, as can be observed in Fig. 7, the rectifier stays at 4-pulse mode and never gets into 2-pulse mode at this phase angle. Another interesting case is at $\phi = 60°$ where 4-pulse mode does not exist and the current unbalance factor increases linearly all the way to 100%.

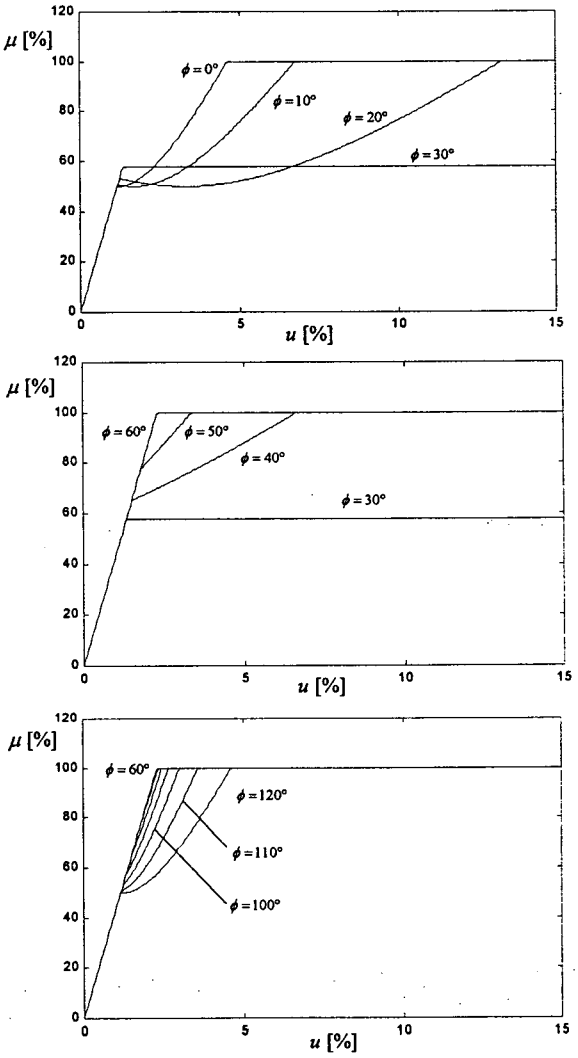

Fig. 12 Current unbalance factor vs. voltage unbalance factor

Fig. 13 is the three-dimensional representation of Fig. 12 showing the variation of the current unbalance factor versus the complex voltage unbalance factor. The figure clearly shows a distinction between the 6-pulse, 4-pulse, and 2-pulse mode that appear as the corn-shaped part at the center, three valleys, and three flat areas at the top, respectively.

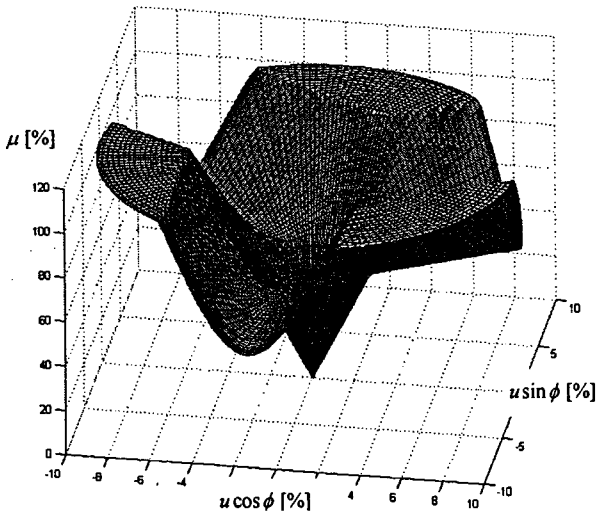

Fig. 13 Current unbalance factor vs. complex voltage unbalance factor

To confirm the validity of the analytical results given above, simulation is carried out with MATLAB/SIMULINK. With simulated line current waveforms of a three-phase diode rectifier for various operating conditions, the fundamental current unbalance factor is calculated and is shown in Fig. 14. For clarity, only the results for $\phi = 0°$ and 60° are shown. It is obvious that theoretical curves generally show good agreement with simulation results.

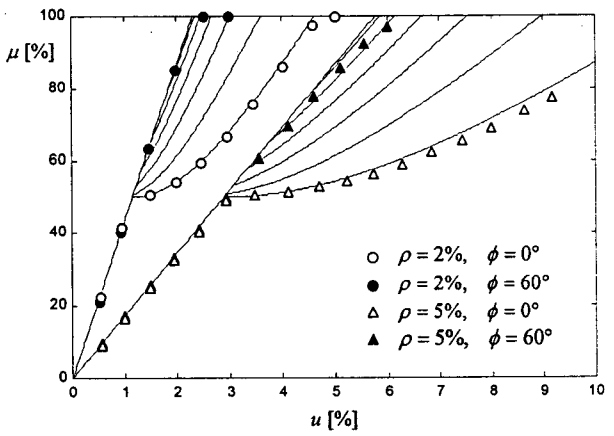

Fig. 14 Simulation results with theoretical prediction

VII. CONCLUSION

This paper gives an analysis of the line current characteristics of a diode rectifier under unbalanced line voltages. It is shown that the line voltage phasors lie on circular loci centered at balanced phasor locations for usual voltage unbalance factor of a few percent. This greatly simplifies the representation of the output voltage variation of the rectifier, which gives the condition of seven distinct operating modes of the rectifier in terms of the voltage unbalance factor and voltage droop ratio that represents combinational effects of the filter reactance and load current.

In each mode of operation, analytical formulas of symmetrical components of fundamental line currents and current unbalance factor are derived. They show that the negative-sequence current and the current unbalance factor are highly sensitive to the voltage unbalance while positive-sequence current is not affected by the voltage unbalance.

The analysis is based on the following assumptions:

1. The voltage unbalance is relatively low
2. Capacitor charging period is very short
3. Effects of line-side reactance are negligible

The first assumption seems to be valid in most practical situations as the voltage unbalance factor is usually restricted within 2-3%. The second assumption implies that the filter capacitor is sufficiently large and/or the load current is small. Therefore, the analysis is valid only when the voltage droop ratio, or the ripple factor in balanced case is relatively low. Simulation results show that the analytical predictions for the voltage droop ratio of less than 5 % are largely acceptable.

The third assumption can be met if the capacity of the rectifier is far smaller than the short circuit capacity of the supply network. The line inductances normally encountered in distribution network may cause the current unbalance to be considerably less sensitive to the voltage unbalance than predicted in this paper. Nevertheless, the approach made in this paper can be justified in that it provides a figure of worst-case, theoretical maximum of current unbalance in an analytical manner, which is useful in designing the supply system for a rectifier or assessing the impact of voltage unbalance on power quality of an existing network feeding rectifier loads.

REFERENCES

[1] G. A. Conway and K. I. Jones, "Harmonic currents produced by variable speed drives with uncontrolled rectifier inputs," Proc. IEE Colloquium on Three-Phase LV Industrial Supplies: Harmonic Pollution and Recent Developments in Remedies, 1993, 4/1-4/5.

[2] M. Grotzbach and J. Xu, "Noncharacteristic line current harmonics in diode rectifier bridges produced by network asymmetries," Rec. of 1993 European Power Electronics Conf., pp.64-69.

[3] M. Bauta and M. Grotzbach, "Noncharacteristic line harmonics of AC/DC converters with high DC current ripple," IEEE Trans. on Power Delivery, vol.15, no.3, pp.1060-1066, July 2000.

[4] E. R. Collins, A. Mansoor, "Effects of voltage sags on AC motor drives," IEEE 1997 Annual Textile, Fiber, and Film Industry Technical Conf., pp.1-7.

[5] A. Fratta, M. Pastorelli, A. Vagati and F. Villata, "Comparison of power supply topologies for industrial drives, based on safety and EMC European standards or directives," Proc. 8th Meditarranean Electrotech. Conf., 1996, pp.1242-1246.

[6] D. A. Rendusara, A. V. Jouanne, P. N. Enjeti, and D. A. Paice, "Design considerations for 12-pulse diode rectifier systems operating under voltage unbalance and pre-existing voltage distortion with some corrective measures," IEEE Trans. on Industry Applications, Vol. 32, No.6, pp.1293-1303, Nov./Dec. 1996.

[7] Y.. Wnag and L. Pierrat, "Probabilistic modeling of current harmonics produced by an AC/DC converter cunder voltage unbalance," IEEE Trans. on Power Delivery, Vol. 8, No. 4, pp.2060-2066, Oct. 1993.